

This is the accepted manuscript version of the contribution published as:

Budhraj, R., Ding, C., Walter, P., Wagner, S., Reemtsma, T., Sawers, G., Adrian, L.
(2019):

The impact of species, respiration type, growth phase and genetic inventory on absolute metal content of intact bacterial cells

Metallomics **11** (5), 925 - 935

The publisher's version is available at:

<http://dx.doi.org/10.1039/C9MT00009G>

1
2
3 **1 The impact of species, respiration type, growth phase and genetic inventory**
4 **2 on absolute metal content of intact bacterial cells**

Article Online
DOI: 10.1039/C9MT00009G

5
6
7 3 Rohit Budhraj^{1,2}, Chang Ding¹, Philipp Walter¹, Stephan Wagner³, Thorsten Reemtsma³, Gary
8 4 Sawers⁴, Lorenz Adrian^{1,2*}

9
10
11
12 ¹Helmholtz Centre for Environmental Research – UFZ, Isotope Biogeochemistry, Leipzig, Germany

13 ²Chair of Geobiotechnology, Technische Universität Berlin, Berlin, Germany

14 ³Helmholtz Centre for Environmental Research – UFZ, Department of Analytical Chemistry, Leipzig,
15 Germany

16 ⁴Institute of Biology/ Microbiology, Martin-Luther Universität, Halle, Germany

17
18
19
20
21
22
23 *To whom correspondence should be addressed: Lorenz Adrian, Helmholtz Centre for Environmental
24 Research – UFZ, Isotope Biogeochemistry, Permoserstraße 15, 04318 Leipzig, Germany, Tel.: +49 (0)
25 341 235 1435, Fax: +49 (0) 341 235 1443, E-Mail: lorenz.adrian@ufz.de

26
27
28
29
30
31
32
33
34
35
36
37
38
39
40
41
42
43
44
45
46
47
48
49
50
51
52
53
54
55
56
57
58
59
60
Keywords: metallome, metalloproteomics, anaerobic respiration, microbes, ICP-MS

17 Abstract

View Article Online
DOI: 10.1039/C9MT00009G

18 Metal ions are abundant in microbial proteins and have structural, catalytic or electron-transferring
19 roles. Metalloproteins are especially prevalent in respiratory chains where they couple electron flow
20 with proton translocation across the membrane. Here, we explore the hypothesis that anaerobic
21 respiratory chains can be investigated by quantitative whole-cell metallomics of the key metals Fe, Co,
22 Ni and Mo. Sensitive and strictly quantitative data were obtained by inductively-coupled plasma mass
23 spectrometry when using a triple quadrupole instrument (ICP-QqQ-MS). Our experiments provide
24 data on the absolute cellular metal content of *E. coli*, an enrichment culture of "*Ca. Kuenenia*
25 *stuttgartiensis*", *Dehalococcoides mccartyi*, *Desulfovibrio vulgaris*, *Geobacter sulfurreducens* and
26 *Geobacter metallireducens*. A major obstacle in whole-cell metallomics is the interference caused by
27 metal precipitates, observed for *G. metallireducens* and *D. vulgaris*. In the other investigated
28 organisms, whole-cell metallomics gave biologically meaningful information, e.g. high Fe and Co
29 content in "*Ca. K. stuttgartiensis*" and higher Mo content in *E. coli* when grown under nitrate-reducing
30 conditions. The content of all four metals was almost constant in *E. coli* from the late exponential
31 phase allowing precise measurements independent of the exact duration of cultivation. Deletion or
32 overexpression of genes involved in metal homeostasis (Ni transport or Mo-cofactor metabolism) was
33 mirrored by dramatic changes in whole-cell metal content. Deletion of genes encoding abundant
34 metalloproteins or heterologous overexpression of metalloproteins was also reflected in the whole-cell
35 metal content. Our study provides a reference point for absolute microbial metallomics and paves the
36 way for the development of fast and easy mutation screens.

37 Significance to metallomics

38 Metallomics looks at the broad and complex roles metals play in biology. Here, we determine absolute
39 numbers of the transition metals Fe, Co, Ni and Mo in bacteria that use different anaerobic respiratory
40 growth modes. The study shows in quantitative terms that different bacterial genera have different
41 overall metal contents. We also show that whole-cell metallomics can provide information about the
42 growth phase, the respiratory mode and the gene inventory of a cell.

43 Introduction

44 Transition metals are abundant in microbial proteins^{1, 2} with intracellular concentrations of combined
45 free and bound species spanning the pico- to micromolar range.³ They play roles in the stabilization of
46 the three-dimensional protein structure, in electron transfer within proteins or in catalysis.^{4, 5} In large
47 respiratory multisubunit protein complexes metal ions are highly organized to form electrically
48 conductive 'wires' through the proteins. Whereas the electron path through proteins is mostly formed
49 by iron-sulfur clusters, the electron entry and exit points are often formed by specialized metal
50 clusters^{6, 7} characterized by the presence of transition metal cations with an incomplete *d*-shell, and
51 which occur in two or more redox-states, such as Fe, Co, Ni, Cu or Mo. In biological systems cysteine
52 residues of the protein backbone often contribute to the coordination of Fe and Ni to form redox-active
53 FeS or NiFeS clusters⁸. Other redox-active metal centers are formed by metal-containing organic
54 cofactors such as heme, cobalamin, cofactor F₄₃₀, and molybdopterin for the metals Fe, Co, Ni and
55 Mo, respectively. These metal-containing cofactors have key functions, for example in cytochromes,
56 organohalide reductive dehalogenases, archaeal methyl-CoM reductase and nitrate reductase, all
57 enzymes involved in anaerobic electron transfer processes. Copper, in contrast, is best known for its
58 involvement in cytochrome oxidase (complex IV) of mitochondrial, bacterial and archaeal respiratory
59 chains. It functions together with heme cofactors in the final oxidation of cytochrome with oxygen,⁹
60 and therefore is more involved in aerobic respiration. The same is true for the copper-containing
61 quinoprotein amine oxidase from *E. coli*.¹⁰ Copper metalloproteins are hypothesized to have appeared
62 late in evolution as an adaptation to oxygen accumulation in the atmosphere.¹¹

63 In anaerobic respiratory chains iron plays a more specific function e.g. in the formation of nickel-iron
64 clusters in [NiFe] hydrogenases or in the active center of iron-only hydrogenases.¹² In the exceptional
65 organisms *Ferroplasma acidiphilum*, iron is found in up to 86% of all cellular proteins.¹³ Cobalt has
66 been detected in many methyltransferases and mutases¹⁴ and plays a major role in the terminal
67 reductases in organohalide respiration. Nickel is crucial in many hydrogenases,^{8, 15} urease, carbon
68 monoxide dehydrogenase (CODH) and acetyl-CoA synthase (ACS). Prokaryotic formate
69 dehydrogenases contain molybdenum complexed as molybdenum *bis* molybdopterin guanine
70 dinucleotide (Mo-*bis*-MGD).⁶ Molybdenum is also involved in terminal reductases of respiratory
71 chains including nitrate, selenate, thiosulfate, polysulfide, tetrathionate, dimethylsulfoxide (DMSO),
72 and trimethylamine oxide (TMAO) reductases.¹⁶

73 Metal homeostasis within microbial cells is maintained by a large number of different proteins with
74 various functions including low- and high-affinity binding, active or passive transport across the cell
75 membrane, storage, incorporation into metal clusters and redox-conversions and several studies on
76 whole-cell metallomics have been published.¹⁷⁻¹⁹ Over the last decades comprehensive analyses have

1
2
3 77 been done to identify deletion mutants impaired in specific parts of metal homeostasis and the
4 78 functions of many proteins have been reported. However, the detection of such mutants is laborious
5
6 79 and relies on biochemical and/or physiological tests. The heterologous overexpression of
7
8 80 metalloproteins represents a major experimental challenge and has only recently been resolved, for
9
10 81 example, for the [NiFe] hydrogenase²⁰⁻²⁴ and cobalt-containing reductive dehalogenases²⁵⁻²⁷ but metal
11
12 82 incorporation has to be tested separately. In this respect, development of a complementary method to
13
14 83 assess the overall metal content of cells, and giving an indication of the consequences of gene
15
16 84 deletions or overexpression would be highly beneficial. A prerequisite for such an approach is that the
17
18 85 deletion mutant affects strongly the overall metal content of a cell or that a heterologously expressed
19
20 86 metalloprotein is present in large amounts to induce significant changes in the total cellular metal
21
22 87 content.

23
24
25
26
27
28
29
30
31
32
33
34
35
36
37
38
39
40
41
42
43
44
45
46
47
48
49
50
51
52
53
54
55
56
57
58
59
60
61
62
63
64
65
66
67
68
69
70
71
72
73
74
75
76
77
78
79
80
81
82
83
84
85
86
87
88 Here, we tested the hypothesis that the growth state of an organism, its respiration mode and its
89
90 genomic complement can be traced via whole-cell metallomics. We focused on *E. coli* as a model
91
92 organism to study the metal content of Fe, Co, Ni and Mo in different growth phases, under different
93
94 respiration regimes and in several mutants impacting metal homeostasis. We then compared the *E. coli*
95
96 results with those obtained for microorganisms with alternative anaerobic metabolic modes, i.e.
97
98 anaerobic ammonium oxidation (anammox), organohalide respiration, metal respiration, nitrate
99
100 respiration and sulfate respiration. Anaerobic ammonium oxidation is a process in which ammonium
101
102 and nitrite are used as electron donor and electron acceptor, respectively, in an anaerobic respiration
103
104 and is catalyzed by specialized organisms. Here we used an enrichment of the anammox bacterium
105
106 *Candidatus* Kuenenia stuttgartiensis which we cultivate in planktonic form in our laboratory.²⁸
107
108 Anammox bacteria are known to contain a high number of heme proteins.²⁹ In organohalide, metal,
109
110 nitrate, fumarate and sulfate respiration halogenated organic compounds, metals, nitrate, fumarate or
111
112 sulfate ions are used as the terminal electron acceptor in an anaerobic respiration while hydrogen or
113
114 other reduced compounds are used as electron donor. In our study we used *Dehalococcoides mccartyi*
115
116 strain CBDB1 as organohalide-respiring bacteria, *Geobacter metallireducens* as metal or nitrate-
117
118 respiring bacteria, *Geobacter sulfurreducens* as fumarate-reducing bacteria and *Desulfovibrio vulgaris*
119
120 as sulfate-reducing bacteria. All measurements were related to the number of cells, allowing us to
121
122 obtain a general parameter for each cell type, which included both metals bound to proteins and metals
123
124 not bound to proteins, present either as free ions or as precipitates within the cell.

107 **Material and Methods**

108 **Chemicals and strain collection**

109 All aqueous dilutions, cultivation media and ICP-MS solutions were prepared with ultrapure water
110 (Millipore, Darmstadt, Germany). Nitric acid (65%, Suprapur) was purchased from Merck (Darmstadt,

1
2
3 111 Germany). ICP multi-element standard solution XVI was obtained from Merck (Darmstadt, Germany)
4 112 and the rhodium internal standard from Fluka. All the other necessary chemicals and solvents were
5 113 purchased from Merck-Aldrich (Germany) in the highest available quality.

6
7 114 *E. coli* strains BW25113 (DSM-27469) and MC4100 (DSM-6574), *Desulfovibrio vulgaris* strain
8 115 Hildenborough number (DSM-644), *Geobacter sulfurreducens* (DSM-12127) and *Geobacter*
9 116 *metallireducens* strain GS-15 (DSM-7210) were obtained from the German Collection of
10 117 Microorganisms and Cell Cultures (DSMZ, Braunschweig, Germany). "*Ca. Kuenenia stuttgartiensis*"
11 118 culture WD²⁸ and *Dehalococcoides mccartyi* strain CBDB1³⁰ are routinely cultivated in our laboratory.
12 119 *E. coli* mutant strains used in this study are described in Table 1.

120 **Bacterial cultivation**

13 121 Our trace element stock solution (1000×) contained 10 mL L⁻¹ HCl (25% v/v), FeCl₂·4H₂O (7.55
14 122 mM), CoCl₂·6H₂O (0.79 mM), MnCl₂·4H₂O (0.5 mM), ZnCl₂ (0.51 mM), H₃BO₃ (0.1 mM),
15 123 Na₂MoO₄·2H₂O (0.15 mM), NiCl₂·6H₂O (0.11 mM), CuCl₂·2H₂O (0.1 mM). Se/W stock solution
16 124 (1000×) contained Na₂SeO₃·5H₂O (22.81 μM), Na₂WO₄·2H₂O (24.25 μM) and NaOH (12.5 mM). Our
17 125 vitamin-4 stock solution (1000×) contained D-biotin (5 mg L⁻¹), thiamine chloride-hydrochloride (50
18 126 mg L⁻¹), dicyanocobinamide (5 mg L⁻¹), dimethylbenzimidazole (5 mg L⁻¹). Luria Bertani Broth (LB
19 127 medium) contained 0.1 g L⁻¹ yeast extract, 0.1 g L⁻¹ tryptone and 50 mg L⁻¹ NaCl and was adjusted to
20 128 pH 7.0 with HCl. The minimal medium contained 10 mM (NH₄)₂SO₄, 10 mM NaCl, 22 mM KH₂PO₄,
21 129 48 mM Na₂HPO₄, 1 mM MgSO₄, 0.1 mM CaCl₂, 25 mM glucose, 1× trace element solution and 1×
22 130 vitamin-4 solution. All anaerobic media were flushed with 20:80 N₂/CO₂ gas mix. The glucose stock
23 131 solution and the vitamin-4 solution were filter-sterilized, and all other solutions were sterilized
24 132 individually by autoclaving.

25 133 Aerobic cultivation of *E. coli* was done in 250 mL Erlenmeyer flasks with 100 mL of LB³¹ or mineral
26 134 medium, as described above, 37°C at 180 rpm on a rotary shaker. Anoxic cultivation of *E. coli* was
27 135 done in nitrogen-gassed minimal medium (MM) with 20 mM KNO₃ as terminal electron acceptor in
28 136 injection bottles closed with butyl septa and crimp caps. Samples of 1 mL were taken from *E. coli*
29 137 cultures for metal analysis after 8, 10, 11, 13, 15, 17, 19, 21, 23, 33 and 48 h of incubation. Cells were
30 138 harvested when the culture reached an OD₆₀₀ of 1.0-1.2. When required, antibiotics were
31 139 supplemented at the following final concentrations: ampicillin, 100 mg L⁻¹, chloramphenicol, 15
32 140 mg L⁻¹, and kanamycin, 25 mg L⁻¹.

33 141 *Dehalococcoides mccartyi* strain CBDB1 was grown in defined cysteine-reduced, bicarbonate-
34 142 buffered, mineral medium with hydrogen as electron donor, 1,2,4,5 tetrabromobenzene as electron
35 143 acceptor and 5 mM acetate as carbon source under strict anoxic conditions as described^{32, 33}. The
36 144 medium contained 1× vitamin-4 and 1× trace element solutions. Cultures were incubated statically
37 145 under strict anoxic conditions at 30°C. Cultures attained cell numbers of approximately 10⁸ cells mL⁻¹.

1
2
3 146 *Desulfovibrio vulgaris* strain Hildenborough was grown in defined anoxic liquid medium containing
4 147 1.5 mM K₂HPO₄, 5 mM NH₄Cl, 17.1 mM NaCl, 2 mM MgCl₂, 7 mM KCl, 1 mM CaCl₂, 1× vitamin-4
5 148 solution, 1× trace element solution, 1× Se/W solution, 4 mM cysteine as a reducing agent, Na-
6 149 resazurin solution (0.1% w/v), 17 mM sodium lactate as electron donor and 11 mM K₂SO₄ as electron
7 150 acceptor. The pH of the medium was adjusted to 7.2 with 1 N HCl. Cultures were grown statically at
8 151 30°C under strict anoxic conditions.

9
10
11 152 *Geobacter sulfurreducens* was cultivated in defined anoxic liquid medium (28 mM NH₄Cl, 4.2 mM
12 153 Na₂HPO₄, 1.35 mM KCl, 30 mM NaHCO₃, 1× vitamin-4 solution, 1× trace element solution, 1× Se/W
13 154 solution, 10 mM Na acetate as carbon source and electron donor and 50 mM sodium fumarate as
14 155 electron acceptor. The cultures were incubated at 30°C under strict anoxic conditions.

15 156 *Geobacter metallireducens* was cultured at 30°C under strictly anoxic conditions in a mineral salt
16 157 medium containing 30 mM acetate as carbon and electron source and 15 mM Fe(III)-citrate as electron
17 158 acceptor as described previously.³⁴ *G. metallireducens* was also cultivated in a modified medium
18 159 where 15 mM Fe(III)-citrate was replaced by 3 mM sodium nitrate and 1 mM Fe(III)-citrate. Cells
19 160 were harvested when the culture medium became clear, indicating depletion of Fe³⁺.

20 161 "*Ca. Kuenenia stuttgartiensis*" was cultivated in a highly enriched mixed culture with approximately
21 162 87% purity in a semi-continuous reactor as described.²⁸ The medium contained synthetic medium with
22 163 20 mM nitrite, and 20 mM ammonium, and 1× trace element solution but without organic carbon
23 164 sources.²⁸ Cells were growing in a planktonic form and were harvested directly from the effluent of the
24 165 reactor.

25 166 **Harvesting and cell counting**

26 167 A volume of 100–200 mL with a cell density of about 10⁸ cells mL⁻¹ was collected for *D. mccartyi*, *D.*
27 168 *vulgaris*, *G. sulfurreducens* and *G. metallireducens* cultures and centrifuged under anoxic conditions
28 169 at 6000 g and 16°C for 60 min. *E. coli* cultures were harvested by centrifugation at 6000 g and 16°C
29 170 for 30 min. All cell pellets were washed twice with 10 mL PBS (phosphate buffered saline, pH 7.2;
30 171 137 mM NaCl, 2.7 mM KCl, 10 mM Na₂HPO₄, 1.8 mM KH₂PO₄) and re-suspended in PBS for metal
31 172 analysis. *G. metallireducens* and "*Ca. Kuenenia stuttgartiensis*" cells were harvested using Percoll
32 173 silica particle beads (Pharmacia) as described in the manufacturer's instruction. Briefly, 6 ml of the
33 174 Percoll suspension were mixed with 3 ml PBS and the mixture was centrifuged at 10,000 g for 30 min.
34 175 About 20–40 ml of a culture with 5 × 10⁷ cells mL⁻¹ was concentrated to a final volume of 1 ml by
35 176 centrifugation at 6000 g for 20 min. This suspension was gently applied onto the top of the gradient
36 177 (total volume 10 mL) and the top half of the density gradient was gently mixed with the cell
37 178 suspension (from 7 – 10 mL). This was followed by a centrifugation step for another 30 min at 6000 g.
38 179 Iron particles settled to the pellet whereas *G. metallireducens* cells were distributed all over in the
39 180 solution. The supernatant (around 8 mL) was diluted to 50 mL with PBS and centrifuged for 30 min at
40 181 6000 g. Around 45 mL of supernatant was discarded and the washing step was repeated again. For

1
2 182 "*Ca. Kuenenia stuttgartiensis*", a bright red band appeared at the lower part of the falcon tube. The
3 bright red band was collected separately and washed twice with PBS. Cell pellets were further re-
4 bright red band was collected separately and washed twice with PBS. Cell pellets were further re-
5 suspended in PBS for metal analysis.
6

7 185 Cells were quantified by direct cell counting using epifluorescence microscopy as described earlier.³⁵
8 Briefly, 20 μL of cell suspension were incubated with 1.3 μL of SYBR Green I (Invitrogen, USA)
9 (1:10000 dilution) in the dark at room temperature for 10 min. Eighteen μL of this suspension were
10 (1:10000 dilution) in the dark at room temperature for 10 min. Eighteen μL of this suspension were
11 added to an agarose-coated slide and immediately covered with a coverslip. Ten to fifteen images were
12 taken with a camera mounted on the epifluorescence microscope and automatically counted via
13 ImageJ and Microsoft Excel macros.³⁵ The sensitivity of this method is at about 10^6 cells mL^{-1} and the
14 standard deviation around 10%.
15
16
17
18
19
20

192 Metal analysis

21 Cell suspensions of 500 μL were subjected to acidic digestion by adding 100 μL of concentrated (65%
22 wt/vol) HNO_3 and incubated at 80°C in an ultrasonic water bath for 2 h. Samples were then diluted
23 with ultrapure water to a final concentration of 2% of HNO_3 . Rhodium internal standard solution was
24 added to a final concentration of $1 \mu\text{g L}^{-1}$ to all samples. ICP multi-element standard solution Merck
25 XVI was serially diluted in 2% HNO_3 to prepare calibration standards between 5 ng L^{-1} and $500 \mu\text{g L}^{-1}$
26 and also amended with the internal $1 \mu\text{g L}^{-1}$ rhodium standard. Samples were measured on a high
27 resolution 8800 ICP-QqQ-MS (Agilent Technologies, USA) in direct infusion mode using an
28 integrated auto-sampler at nebulizer speed of 0.3 rps (revolutions per second) and internal tube
29 diameter of 1.02 mm for 45 s. The five metals Fe, Co, Ni, Mo and Rh were quantified. All
30 measurements were performed in three technical replicates normalized with the internal standard and
31 averaged by taking the mean value. All statistical analysis was performed using student t-test. We
32 report our data as metal ions per cell because we can directly determine the amount of metal ions by
33 ICP-MS and the microbial cell number by direct cell counting. When numbers of ions are reported it is
34 meant to include the total amount of all chemical species of an element in a given sample including
35 charged ions and uncharged atoms.
36
37
38
39
40
41
42
43
44

45 To reduce polyatomic interferences, especially from ArO and NaCl which have the same nominal
46 mass of 56 as Fe and 60 as Ni, respectively, we used the Octopole Reaction System (ORS³) with a
47 collision/reaction cell (CRC). Hydrogen was added to the CRC at a flow rate of 3.0 mL min^{-1} . For all
48 metals, the target masses of the first (Q1) and second (Q2) quadrupole were set to the same m/z value:
49 Fe (56/56), Co (59/59), Ni (60/60), Mo (95/95) and Rh (103/103) with an integration time of 1 s under
50 auto-detector mode. H_2 gas was introduced through the 2nd inlet line and argon gas (Ar) was added as a
51 carrier gas via a dilution gas port located between the torch and the spray chamber. A Peltier-cooled
52 (2°C) Scott-type spray chamber with a perfluoroalkoxy alkane (PFA) nebulizer was used as the
53 injection system. All other parameters were optimized by the auto-tune function of the used ICP-MS
54
55
56
57
58
59
60

217 MassHunter 4.2 workstation software. Further instrument operation parameters are given in
218 Supplementary Table 1.

View Article Online
DOI: 10.1039/C9MT00009G

219 Results

220 Metal determination at nanomolar concentrations by ICP-MS

221 Calibration curves for the four target metals Fe, Co, Ni and Mo measured at 14 different
222 concentrations from 5 ng L⁻¹ to 500 µg L⁻¹ in triplicate showed excellent linearity ($R^2 = 0.99$) for all
223 four metals, confirming the applicability of the instrument. Such exact correlations with metal
224 concentrations down to 20 pM for ⁶⁰Ni, 260 pM for ⁹⁵Mo and in the nanomolar range for ⁵⁶Fe and ⁵⁹Co
225 (Table 2) were only achieved using hydrogen in the collision/reaction cell to reduce polyatomic
226 interferences, but not using He as a collision gas or without gas. All further measurements were done
227 with hydrogen in the reaction cell.

228 Metal analysis of whole cells

229 Relating ICP-MS measurements for Fe, Co, Ni, and Mo to the number of cells resulted in absolute
230 numbers of metal ions per cell (Fig. 1). The absolute amount of Fe ions per untreated cell were
231 between 6.78×10^5 for *D. mccartyi* and 1.08×10^{10} for *G. metallireducens*. Because we speculated
232 that a large part of the Fe in *G. metallireducens* is enclosed in iron-containing abiotic particles we also
233 analyzed *G. metallireducens* after centrifugation in a Percoll density gradient. This resulted in a
234 number of 1.22×10^8 ions per cell, which were 2 orders of magnitude lower than without Percoll
235 gradient washing. Nevertheless, the amounts of Fe ions per cell in *G. metallireducens* remained up to
236 eight times higher than in "*Ca. Kuenenia stuttgartiensis*" (1.6×10^7) and in *G. metallireducens* grown
237 under nitrate conditions (1.4×10^7), more than 30-fold higher than in *G. sulfurreducens* (3.9×10^6) and
238 12-fold higher than in aerobically grown *E. coli* in minimal medium (9.7×10^6). *E. coli* grown
239 aerobically and anaerobically in mineral medium, together with *D. vulgaris*, had similar Fe contents of
240 about 1×10^7 ions per cell. The highest amount of Ni ions per cell was observed in "*Ca. Kuenenia*
241 *stuttgartiensis*" (1.6×10^5). Among all the analyzed bacteria, the amount of Co was maximal in *E. coli*
242 grown aerobically (1.6×10^5) and anaerobically in minimal medium (2.3×10^5). The lowest amount of
243 Co determined in the investigated bacterial species was observed with *E. coli* grown in LB medium.
244 We observed the highest amount of Mo *D. vulgaris* (3.3×10^5 ions per cell) and the lowest in *E. coli*
245 grown under aerobic conditions with LB medium (1.5×10^4) and in *G. metallireducens* grown with
246 Fe(III) citrate as electron acceptor (1.8×10^4). *E. coli* grown under nitrate-reducing conditions in
247 minimal medium contained 2.5-fold more Mo (5.0×10^4 ions per cell) than cells grown in the presence
248 of oxygen (2.0×10^4 ions per cell).

249 **Metal content in different growth phases**

View Article Online
DOI: 10.1039/C9MT00009G

250 To be able to correlate the metal content of a cell in batch culture to its physiology and the mode of
251 respiration it uses, the metal content must be stable across all growth stages of a culture. To test if this
252 was the case, we analyzed the content of all our four target metals in *E. coli* strain BW25113 in
253 aerobic LB medium over a total incubation time of 50 h. As expected, the total concentration of metals
254 bound in bacterial biomass increased with the incubation time (Fig. 2A-C), and this correlated with the
255 increase in biomass (data not shown). When relating the biomass-bound metal concentrations to the
256 cell numbers in the cultures the amounts of all four target metals per cell were essentially constant
257 from 8 h of growth. This time point corresponded with the entry of the bacteria into the early
258 stationary phase (Fig. 2D). Metal analysis from the exponential phase did not lead to consistent data.

259 ***E. coli* mutant analysis**

260 We then tested if metal analysis of whole cells can provide information about the genetic inventory of
261 a cell. For this we focused on Ni and Mo and analyzed strains carrying two types of mutations: first,
262 deletion mutants affected in their ability to transport or to incorporate specifically into proteins either
263 Ni or Mo. This was achieved by impairing the whole Ni or Mo homeostasis ("systemic mutations");
264 and second, mutants lacking a specific nickel- or molybdenum-containing enzyme, which was
265 achieved by deleting the gene encoding the corresponding Ni- or Mo-cofactor-containing subunit
266 ("structural mutations"). In structural mutants only specific metalloproteins were deleted or
267 overexpressed and we hypothesized that in such mutants the overall effect on metal-content should be
268 lower than in systemic mutants.

269 *E. coli* strains with the systemic knockout mutations in *nikC* or *nikE*, both involved in Ni transport, or
270 in *fnr*, a transcription factor required for expression of genes for both nickel transport as well as for
271 hydrogenase,³⁶ contained significantly lower total amounts of Ni per cell than the *E. coli* wild-type
272 BW25113 (Fig. 3A). Deletion of *moaA*, encoding a protein catalyzing the first step of molybdopterin
273 biosynthesis, strongly reduced the total Mo content in *E. coli* cells compared to the wild-type. This
274 was true for aerobic cultivation on two different media, but also under nitrate-reducing conditions and
275 exclusion of oxygen (Fig. 3B).

276 A reduction of the Ni-content by about 33% in comparison to the wild-type was found for the mutant
277 FTD147, which lacks the catalytic subunit of three [NiFe] hydrogenases in *E. coli* (Fig. 4A). In
278 contrast, mutants of FTD147 in which the HybC, the large subunit of [NiFe] hydrogenase, was
279 overproduced, was not reduced in Ni-content.

280 In wild-type *E. coli* MC4100 we observed about 2.5-fold higher Mo-content under nitrate-reducing
281 conditions (5×10^4) than under aerobic conditions (2×10^4) (Fig. 4B). Deletions in genes for several
282 subunits of the hydrogenase ($\Delta hypB$, $\Delta hypC$, $\Delta hypE$), $\Delta hyfB-R$ and translation factor ($\Delta selB$) resulted
283 in a slightly lower Mo-content under aerobic conditions compared to the wild-type but in a strongly

1
2 284 reduced Mo-content under nitrate-reducing conditions compared to the wild-type. When we then
3
4 285 heterologously overexpressed the *omeAB* genes from *Dehalococcoides mccartyi* strain CBDB1,
5
6 286 hypothesized to encode a Mo-containing protein complex, we determined an increase in the mean
7
8 287 level of the cellular Mo-content under both tested conditions. (Fig. 4B).
9
10

11 288 **Discussion**

12
13
14 289 The highly specific and sensitive detection of metal ions has been significantly improved within the
15
16 290 last few years due to developments in mass spectrometric instrumentation and data processing. We
17
18 291 demonstrate in this study that mass spectrometric detection using a triple quadrupole can be used for
19
20 292 the quantification of low amounts of metals in complex biological samples. In our experiments, the
21
22 293 best results were obtained by using the Octopole Reaction System as a hydrogen reduction cell to
23
24 294 remove polyatomic interferences rather than using as a collision cell. This strongly reduced the
25
26 295 background and resulted in high sensitivity and a strictly linear response.

27
28 296 We focused on the quantification of respiratory metals in intact cells to test the hypothesis that such
29
30 297 data can give meaningful biological information on major processes within the cell in which the
31
32 298 contributing proteins have either a strong systemic effect on cellular metal homeostasis or are
33
34 299 abundant metalloenzymes. In microorganisms metal ions can be bound to organic molecules but can
35
36 300 also be freely solvated in the cytoplasm or accumulating in abiotic precipitates within the cell or on its
37
38 301 surface.^{37, 38} The fraction of cellular metal ions bound to organic molecules is mainly bound to
39
40 302 proteins, either directly to the amino acid chain or indirectly via a cofactor such as heme, cobalamin,
41
42 303 cofactor F₄₃₀ and NiFe-cofactor, or Mo-*bis*-MGD for Fe, Co, Ni and Mo, respectively. Abiotic
43
44 304 precipitates appeared to be especially abundant in our Fe(III)-reducing model organism *G.*
45
46 305 *metallireducens* grown with Fe(III) citrate as electron acceptor and our sulfate-reducing model
47
48 306 organism *D. vulgaris* grown with sulfate as electron acceptor. Both species appear to form precipitates
49
50 307 that greatly overshadow protein-bound metals. For *G. metallireducens* we could confirm this by
51
52 308 washing Fe precipitates off the cell surface in a Percoll gradient, which revealed that protein-bound
53
54 309 metals make up less than 1% of the total metal content. This was also confirmed by the results after
55
56 310 cultivation of *G. metallireducens* with nitrate as electron acceptor, which prevented the formation of
57
58 311 abiotic iron precipitates. In *D. vulgaris* this effect led to massive accumulation of Mo that could not be
59
60 312 removed by washing of the cells. There is currently limited literature available describing the impact
313
314 313 of intracellular Mo sulfides on the physiology of the cell or on the ecology of populations, as this
315
316 314 should lead to general Mo depletion in sulfide-reducing environments. Taken together, the whole-cell
317
318 315 metallomic data from iron- or sulfate-reducing bacteria must be interpreted with caution.

319
320 316 In contrast, the data from whole-cell metal analysis of bacteria that do not form metal sulfides can be
321
322 317 meaningfully interpreted and can yield important biological insights. For example, the high amount of
323

1
2 318 Fe in "*Ca. Kuenenia stuttgartiensis*" indicates iron plays a crucial and dominant role in the
3
4 319 anammoxosomes of these anammox bacteria.³⁹ The low Fe content of *D. mccartyi* strain CBDB1 is
5
6 320 probably due to its low cell volume, which is reported to be only about 2% of that of *E. coli*.⁴⁰

7
8 321 The highest Co content per cell was observed in *E. coli* grown in minimal medium. The Co-containing
9
10 322 cofactor cobamide cannot be synthesized *de novo* by *E. coli*;²⁵ however, because the cobalamin
11
12 323 precursor cobinamide was added to the mineral medium, cobalamin-containing enzymes could be
13
14 324 nevertheless synthesized, e.g., the B₁₂-dependent methionine synthase, MetH. This enzyme might not
15
16 325 be strongly expressed in LB medium as methionine is directly available to the bacteria. Co is also the
17
18 326 central ion of cobalamin-dependent reductive dehalogenases involved in organohalide respiration in *D.*
19
20 327 *mccartyi*.^{40, 41} However, the absolute number of reductive dehalogenases estimated by mass
21
22 328 spectrometric selective reaction monitoring was determined to be around 500 per cell⁴² and therefore
23
24 329 might not contribute much to the overall determined number of around 10,000 Co ions per cell as
25
26 330 determined by ICP-QQ-MS. This discrepancy needs to be further explored.

27
28 331 By far the highest Ni content was found in "*Ca. Kuenenia stuttgartiensis*". Genomes sequences are
29
30 332 available for the highly enriched strains KUST and MBR1^{43, 44} and indicate the coding capacity for a
31
32 333 Ni transporter (CbiNLMQ), a Ni-containing CO-methylating acetyl-CoA synthase (CODH/ACS)⁴³
33
34 334 and one [NiFe] hydrogenase complex. The activity of CODH/ACS in anammox bacteria was
35
36 335 biochemically demonstrated.⁴⁴ As it is involved in carbon fixation for autotrophic growth it is
37
38 336 anticipated to contribute substantially to the high Ni content in *Kuenenia* species.

39
40 337 As indicated above, the high Mo content in *D. vulgaris* is likely the result of its precipitation as
41
42 338 MoS₂,³⁸ although Mo transport³⁸ and the expression of Mo-cofactor-containing formate
43
44 339 dehydrogenases^{45, 46} has been described for *D. vulgaris*. The fact that Mo precipitates could not be
45
46 340 separated from cells in a Percoll gradient could indicate the intracellular or periplasmic location of
47
48 341 these precipitates or at least their tight association with the cells. Others have suggested that such
49
50 342 Mo(IV)S₂ precipitates are formed after Mo(VI) to Mo(IV) reduction in the periplasm of sulfate-
51
52 343 reducing bacteria.³⁸ With *E. coli* the comparison of the Mo content in cells grown in oxic or anoxic
53
54 344 mineral medium with nitrate as electron acceptor resulted in the expected higher Mo content in
55
56 345 anoxically grown cultures, presumably due to the expression of Mo-containing formate dehydrogenase
57
58 346 and nitrate reductase, which are present in significant abundance in these cells.^{47, 48} These data indicate
59
60 347 that the metal content of *E. coli* accurately reflects the respiration mode used by the bacterium.

348
349 The monitoring of *E. coli* throughout its batch cultivation revealed that the content of all four
350
351 349 investigated metals is remarkably stable from the late exponential phase onwards for over more than
352
353 350 40 hours of incubation. This stability allows a precise comparison of *E. coli* strains in different growth
354
355 351 media as described above, or with different genetic inventories. We could therefore successfully apply
356
357 352 whole-cell analysis to analyze the metal content in mutant strains impacted in Ni or Mo homeostasis.
358
359 353 We expected strong impacts of systemic mutations and lower, but nevertheless significant, changes

1
2 354 due to structural gene mutations encoding abundant metalloproteins. Indeed, the systemic knockout of
3
4 355 Ni-transporter genes ($\Delta nikC$ or $\Delta nikE$) strongly impacted intracellular Ni levels. Similarly, the
5
6 356 knockout of the gene encoding the FNR protein, which is a global regulator necessary, e.g., for
7
8 357 transcription of the Ni-transporter genes,⁴⁹ strongly reduced Ni levels in both tested *E. coli*
9
10 358 cultivations. This confirms earlier descriptions that FNR is the primary regulator for Ni transport but
11
12 359 also shows the power of whole-cell metallomics for the detection of systemic mutations. Even more
13
14 360 pronounced was the reduction of Mo abundance with the systemic knockout of *moaA*. MoaA catalyzes
15
16 361 the first step of molybdopterin biosynthesis⁵⁰ and forms the major route to incorporate Mo into *E. coli*
17
18 362 proteins. The overall low Mo content demonstrates that Mo does not accumulate in the cells if it
19
20 363 cannot be incorporated into its target enzymes. This suggests feedback regulation between transport
21
22 364 and the cofactor biosynthetic pathway⁵¹, however, we can also not exclude an increased efflux.
23
24 365 Residual Mo might have been bound to the transporter, might be freely soluble in the cytoplasm as
25
26 366 molybdate anions or might be unspecifically attached to other cell components.

27
28 367 Strains with knockouts of genes encoding abundant metalloproteins were diminished in their
29
30 368 respective metal content, demonstrating that whole-cell metallomics can be applied to examine the
31
32 369 metal content of single abundant proteins. The overall Ni content in *E. coli* was ~25% lower after the
33
34 370 knockout of a [NiFe] hydrogenases (Hyd-1, 2 and 3), suggesting that ~25% of the total cellular Ni
35
36 371 amount, corresponding to ~2000 ions, was bound to these hydrogenases.³⁶ The fact that the
37
38 372 complementation with HybC restored original Ni levels reveals that the overproduced HybC contains
39
40 373 Ni indicating correct maturation and confirming earlier enzymatic observations.⁴⁹ Moreover, it
41
42 374 confirms that HybC is the Ni-containing subunit, and demonstrates that the Ni transport and storage
43
44 375 system is closely linked to the incorporation of Ni into metalloproteins. Clearly, whole-cell
45
46 376 metallomics can also be used to identify yet-unknown and abundant metalloproteins by screening
47
48 377 mutants for metal content, as was proposed earlier.¹

49
50 378 Finally, we applied whole-cell metallomics to try to answer the question if OmeA, a protein in the
51
52 379 organohalide respiration complex of *D. mccartyi*^{30, 52} with a Mo-bis-MGD-binding site, contains Mo
53
54 380 cofactors when overexpressed in an *E. coli* host. The wild type again showed significantly higher Mo
55
56 381 levels when grown with nitrate compared with when oxygen was the terminal electron acceptor,
57
58 382 indicating that the Mo-containing formate dehydrogenase and nitrate reductase bind about two thirds
59
60 383 of the total cellular Mo under these conditions. The *moaA* knockout strain reduced Mo content
384 significantly, especially under nitrate-reducing conditions. After heterologous overproduction of the
385 OmeAB heterodimer in this mutant strain we observed a small increase in Mo content, which however
386 proved not to be significant. Despite several repetitions of this experiment, no clear increase of the Mo
387 content was observed, although the apoprotein was present in large amounts. We must interpret this
388 data that it indicates that the *E. coli* Mo-cofactor incorporation machinery was ineffective at
389 incorporation of the Mo-cofactor into the heterologously produced protein. This could either be due to

1
2 390 the fact that the heterologously expressed enzyme was misfolded, or that the correctly folded OmeA
3 protein does not bind Mo, as has been described for other metalloproteins with a predicted Mo-*bis*-
4 391 MGD binding site.^{53, 54}
5
6
7
8
9
10
11
12

View Article Online
DOI: 10.1039/C9MT00009G

Metallomics Accepted Manuscript

Published on 01 March 2019. Downloaded by Washington University in St. Louis on 3/12/19 12:01:30 PM.

393 **Conclusion**

394 ICP-QqQ-MS can be applied to obtain absolute quantification of the cellular content of biologically
395 important metals in whole cells at very high sensitivity so that the metal content can be analyzed also
396 from microorganisms for which only low amounts of cell mass is available. The meaningful
397 interpretation of whole-cell metallomics data is possible if no metal precipitates are formed. While we
398 have identified single metalloproteins that contribute a major share of the total amount of a metal
399 within a cell, it would be worth analyzing in detail all contributions of different metalloproteins¹ to the
400 total content of different metals to identify gaps of our knowledge. If further elaborated, the method
401 could be a tool to quantify metalloproteins in a facile, rapid and reliable way. Whole-cell metallomics
402 showed particular strength in tracing the effects of mutations involved in metal homeostasis on the
403 cellular metal content. Whereas systemic mutations, e.g. in metal transport or metal-cluster assembly,
404 are readily identifiable, the consequences of mutations in genes encoding metalloproteins are only
405 detectable if these proteins are abundant and if the metal-binding property of the protein is affected. In
406 summary, whole-cell metabolomics represents a very fast, easy and strictly quantitative approach that
407 can give direct information about the metal homeostasis of a microbial cell.

408 **Conflict of interest**

409 The authors declare that they have no conflict of interest.

410 **Acknowledgements**

411 The authors thank Dr. Jürgen Mattusch for analytical support and Benjamin Scheer for technical
412 support. Stefanie Hartwig and Nadya Dragomirova are thanked for the kind gift of plasmid constructs.
413 This work was funded by the German Research Council (DFG) within the Research Group SPP1927.
414 Protein mass spectrometry was done at the Centre for Chemical Microscopy (ProVIS) at the
415 Helmholtz Centre for Environmental Research, which is supported by European regional development
416 funds (EFRE—Europe Funds Saxony) and the Helmholtz Association.

417 **Author contributions**

418 R.B. and L.A. conceived the study and designed the experiments in coordination with G.S. and S.W.
419 The lab experiments were done by R.B., D.C. and P.W., data was analyzed by R.B. and L.A.. R.B. and
420 L.A. wrote the manuscript, and G.S., D.C., S.W. and T.R. contributed to the interpretation of the data
421 and edited the manuscript.

422 **Literature**

- 423 1. A. Cvetkovic, A. L. Menon, M. P. Thorgersen, J. W. Scott, F. L. Poole Jr, F. E. Jenney Jr, W.
424 A. Lancaster, J. L. Praissman, S. Shanmukh, B. J. Vaccaro, S. A. Trauger, E. Kalisiak, J. V.
425 Apon, G. Siuzdak, S. M. Yannone, J. A. Tainer and M. W. W. Adams, Microbial
426 metalloproteomes are largely uncharacterized, *Nature*, 2010, **466**, 779-782.
- 427 2. Y. Zhang and V. N. Gladyshev, General trends in trace element utilization revealed by
428 comparative genomic analyses of Co, Cu, Mo, Ni, and Se, *J. Biol. Chem.*, 2010, **285**, 3393-
429 3405.
- 430 3. J. Szpunar, Metallomics: a new frontier in analytical chemistry, *Anal. Bioanal. Chem.*, 2004,
431 **378**, 54-56.
- 432 4. D. C. Rees, Great metalloclusters in enzymology, *Ann. Rev. Biochem.*, 2002, **71**, 221-246.
- 433 5. B. Schoepp-Cothenet, R. van Lis, A. Atteia, F. Baymann, L. Capowiez, A.-L. Ducluzeau, S.
434 Duval, F. ten Brink, M. J. Russell and W. Nitschke, On the universal core of bioenergetics,
435 *Biochim. Biophys. Acta - Bioenergetics*, 2013, **1827**, 79-93.
- 436 6. M. Jormakka, S. Tornroth, B. Byrne and S. Iwata, Molecular basis of proton motive force
437 generation: Structure of formate dehydrogenase-N, *Science*, 2002, **295**, 1863-1868.
- 438 7. R. G. Efremov, R. Baradaran and L. A. Sazanov, The architecture of respiratory complex I,
439 *Nature*, 2010, **465**, 441-445.
- 440 8. W. Lubitz, H. Ogata, O. Rüdiger and E. Reijerse, Hydrogenases, *Chemical Reviews*, 2014,
441 **114**, 4081-4148.
- 442 9. T. Tsukihara, H. Aoyama, E. Yamashita, T. Tomizaki, H. Yamaguchi, K. Shinzawa-Itoh, R.
443 Nakashima, R. Yaono and S. Yoshikawa, The whole structure of the 13-subunit oxidized
444 cytochrome c oxidase at 2.8 Å, *Science*, 1996, **272**, 1136-1144.
- 445 10. C. M. Wilmot, J. Hajdu, M. J. McPherson, P. F. Knowles and S. E. V. Phillips, Visualization
446 of dioxygen bound to copper during enzyme catalysis, *Science*, 1999, **286**, 1724-1728.
- 447 11. W. Nitschke, S. E. McGlynn, E. J. Milner-White and M. J. Russell, On the antiquity of
448 metalloenzymes and their substrates in bioenergetics, *Biochimica et Biophysica Acta (BBA) -*
449 *Bioenergetics*, 2013, **1827**, 871-881.
- 450 12. J. W. Peters, G. J. Schut, E. S. Boyd, D. W. Mulder, E. M. Shepard, J. B. Broderick, P. W.
451 King and M. W. W. Adams, [FeFe]- and [NiFe]-hydrogenase diversity, mechanism, and
452 maturation, *Biochimica et Biophysica Acta (BBA) - Molecular Cell Research*, 2015, **1853**,
453 1350-1369.
- 454 13. M. Ferrer, O. V. Golyshina, A. Beloqui, P. N. Golyshin and K. N. Timmis, The cellular
455 machinery of *Ferroplasma acidiphilum* is iron-protein-dominated, *Nature*, 2007, **445**, 91-94.
- 456 14. R. G. Matthews, M. Koutmos and S. Datta, Cobalamin-dependent and cobamide-dependent
457 methyltransferases, *Curr. Opin. Struct. Biol.*, 2008, **18**, 658-666.
- 458 15. P. M. Vignais, B. Billoud and J. Meyer, Classification and phylogeny of hydrogenases, *FEMS*
459 *Microbiol. Rev.*, 2001, **25**, 455-501.
- 460 16. R. A. Rothery, G. J. Workun and J. H. Weiner, The prokaryotic complex iron-sulfur
461 molybdoenzyme family, *Biochim. Biophys. Acta - Biomembranes*, 2008, **1778**, 1897-1929.
- 462 17. P. T. Chivers, E. L. Benanti, V. Heil-Chapdelaine, J. S. Iwig and J. L. Rowe, Identification of
463 Ni-(l-His)₂ as a substrate for NikABCDE-dependent nickel uptake in *Escherichia coli*,
464 *Metallomics*, 2012, **4**, 1043-1050.
- 465 18. A. M. Donnell, S. Lewis, S. Abraham, K. Subramanian, J. L. Figueroa, G. S. Deepe and A. P.
466 Vonderheide, Investigation of an optimal cell lysis method for the study of the zinc
467 metalloproteome of *Histoplasma capsulatum*, *Anal. Bioanal. Chem.*, 2017, **409**, 6163-6172.
- 468 19. A. T. Al-sandaqchi, C. Brignell, J. F. Collingwood, K. Geraki, E. M. Mirkes, K. Kong, M.
469 Castellanos, S. T. May, C. W. Stevenson and H. M. Elsheikha, Metallome of cerebrovascular
470 endothelial cells infected with *Toxoplasma gondii* using μ -XRF imaging and inductively
471 coupled plasma mass spectrometry, *Metallomics*, 2018, **10**, 1401-1414.

- 1
2
3
4
5
6
7
8
9
10
11
12
13
14
15
16
17
18
19
20
21
22
23
24
25
26
27
28
29
30
31
32
33
34
35
36
37
38
39
40
41
42
43
44
45
46
47
48
49
50
51
52
53
54
55
56
57
58
59
60
20. J. Schiffels, O. Pinkenburg, M. Schelden, E.-H. A. A. Aboulhaga, M. E. M. Baumann and T. Selmer, An innovative cloning platform enables large-scale production and maturation of an oxygen-tolerant [NiFe]-hydrogenase from *Cupriavidus necator* in *Escherichia coli*, *PLoS One*, 2013, **8**, e68812.
21. N. Dragomirova, P. Rothe, S. Schwoch, S. Hartwig, C. Pinske and R. G. Sawers, Insights into the redox sensitivity of Chloroflexi Hup-hydrogenase derived from studies in *Escherichia coli*: merits and pitfalls of heterologous [NiFe]-hydrogenase synthesis, *Front. Microbiol.*, 2018, **9**, 2837-2837.
22. S. Hartwig, C. Thomas, N. Krumova, V. Quitzke, D. Türkowsky, N. Jehmlich, L. Adrian and R. G. Sawers, Heterologous complementation studies in *Escherichia coli* with the Hyp accessory protein machinery from *Chloroflexi* provide insight into [NiFe]-hydrogenase large subunit recognition by the HypC protein family, *Microbiology-SGM*, 2015, **161**, 2204-2219.
23. P. D. Weyman, W. A. Vargas, R.-Y. Chuang, Y. Chang, H. O. Smith and Q. Xu, Heterologous expression of *Alteromonas macleodii* and *Thiocapsa roseopersicina* [NiFe] hydrogenases in *Escherichia coli*, *Microbiology*, 2011, **157**, 1363-1374.
24. J. Sun, R. C. Hopkins, F. E. Jenney, Jr., P. M. McTernan and M. W. W. Adams, Heterologous expression and maturation of an NADP-dependent [NiFe]-hydrogenase: a key enzyme in biofuel production, *PLoS One*, 2010, **5**, e10526.
25. A. Mac Nelly, M. Kai, A. Svatoš, G. Diekert and T. Schubert, Functional heterologous production of reductive dehalogenases from *Desulfitobacterium hafniense* strains, *Appl. Environ. Microbiol.*, 2014, **80**, 4313-4322.
26. A. Parthasarathy, T. A. Stich, S. T. Lohner, A. Lesnefsky, R. D. Britt and A. M. Spormann, Biochemical and EPR-spectroscopic investigation into heterologously expressed vinyl chloride reductive dehalogenase (VcrA) from *Dehalococcoides mccartyi* strain VS, *J. Am. Chem. Soc.*, 2015, **137**, 3525-3532.
27. R. Nakamura, T. Obata, R. Nojima, Y. Hashimoto, K. Noguchi, T. Ogawa and M. Yohda, Functional expression and characterization of tetrachloroethene dehalogenase from *Geobacter* sp, *Front. Microbiol.*, 2018, **9**.
28. C. Ding, F. O. Enyi and L. Adrian, Anaerobic ammonium oxidation (anammox) with planktonic cells in a redox-stable semicontinuous stirred-tank reactor, *Environ. Sci. Technol.*, 2018, **52**, 5671-5681.
29. B. Kartal and J. T. Keltjens, Anammox biochemistry: A tale of heme c proteins, *Trends Biochem. Sci.*, 2016, **41**, 998-1011.
30. K. Seidel, J. Kühne and L. Adrian, The complexome of *Dehalococcoides mccartyi* reveals its organohalide respiration-complex is modular, *Front. Microbiol.*, 2018, **9**, 1130.
31. J. Sambrook, E. F. Fritsch and T. Maniatis, *Molecular cloning: a laboratory manual*, Cold Spring Harbor Laboratory Press, Cold Spring Harbor, NY, 1989.
32. C. J. Schipp, E. Marco-Urrea, A. Kublik, J. Seifert and L. Adrian, Organic cofactors in the metabolism of *Dehalococcoides mccartyi* strains, *Philos. Trans. R. Soc., B*, 2013, **368**.
33. G. Jayachandran, H. Görisch and L. Adrian, Dehalorespiration with hexachlorobenzene and pentachlorobenzene by *Dehalococcoides* sp strain CBDB1, *Arch. Microbiol.*, 2003, **180**, 411-416.
34. D. R. Lovley and E. J. P. Philips, Novel mode of microbial energy metabolism: organic carbon oxidation coupled to dissimilatory reduction of iron or manganese, *Appl. Environ. Microbiol.*, 1988, **54**, 1472-1480.
35. L. Adrian, S. K. Hansen, J. M. Fung, H. Görisch and S. H. Zinder, Growth of *Dehalococcoides* strains with chlorophenols as electron acceptors, *Environ. Sci. Technol.*, 2007, **41**, 2318-2323.
36. C. Pinske and R. G. Sawers, Anaerobic formate and hydrogen metabolism, *EcoSal Plus*, 2016, **7**.
37. C. Zhou, R. Vannela, K. F. Hayes and B. E. Rittmann, Effect of growth conditions on microbial activity and iron-sulfide production by *Desulfovibrio vulgaris*, *J. Hazard. Mater.*, 2014, **272**, 28-35.
38. K. C. Biswas, N. A. Woodards, H. Xu and L. L. Barton, Reduction of molybdate by sulfate-reducing bacteria, *BioMetals*, 2009, **22**, 131-139.

- 1
2 527 39. L. van Niftrik, W. J. Geerts, E. G. van Donselaar, B. M. Humbel, A. Yakushevska, A. J.
3 528 Verkleij, M. S. Jetten and M. Strous, Combined structural and chemical analysis of the
4 529 anammoxosome: a membrane-bounded intracytoplasmic compartment in anammox bacteria,
5 530 *Journal of Structural Biology*, 2008, **161**, 401-410. View Article Online
DOI: 10.1016/j.jstb.2008.09.009
- 6 531 40. F. E. Löffler, J. Yan, K. M. Ritalahti, L. Adrian, E. A. Edwards, K. T. Konstantinidis, J. A.
7 532 Müller, H. Fullerton, S. H. Zinder and A. M. Spormann, *Dehalococcoides mccartyi* gen. nov.,
8 533 sp nov., obligately organohalide-respiring anaerobic bacteria relevant to halogen cycling and
9 534 bioremediation, belong to a novel bacterial class, *Dehalococcoidia* classis nov., order
10 535 *Dehalococcoidales* ord. nov and family *Dehalococcoidaceae* fam. nov., within the phylum
11 536 *Chloroflexi*, *Int. J. Syst. Evol. Microbiol.*, 2013, **63**, 625-635.
- 12 537 41. T. Hölscher, H. Görisch and L. Adrian, Reductive dehalogenation of chlorobenzene congeners
13 538 in cell extracts of *Dehalococcoides* sp strain CBDB1, *Appl. Environ. Microbiol.*, 2003, **69**,
14 539 2999-3001.
- 15 540 42. C. Schiffmann, R. Hansen, S. Baumann, A. Kublik, P. H. Nielsen, L. Adrian, M. von Bergen,
16 541 N. Jehmlich and J. Seifert, Comparison of targeted peptide quantification assays for reductive
17 542 dehalogenases by selective reaction monitoring (SRM) and precursor reaction monitoring
18 543 (PRM), *Anal. Bioanal. Chem.*, 2014, **406**, 283-291.
- 19 544 43. J. Frank, S. Lücker, R. H. A. M. Vossen, M. S. M. Jetten, R. J. Hall, H. J. M. Op den Camp
20 545 and S. Y. Anvar, Resolving the complete genome of *Kuenenia stuttgartiensis* from a
21 546 membrane bioreactor enrichment using Single-Molecule Real-Time sequencing, *Sci. Rep.*,
22 547 2018, **8**, 4580.
- 23 548 44. M. Strous, E. Pelletier, S. Mangenot, T. Rattei, A. Lehner, M. W. Taylor, M. Horn, H. Daims,
24 549 D. Bartol-Mavel and P. Wincker, Deciphering the evolution and metabolism of an anammox
25 550 bacterium from a community genome, *Nature*, 2006, **440**, 790-794.
- 26 551 45. C. Sebban, L. Blanchard, M. Bruschi and F. Guerlesquin, Purification and characterization of
27 552 the formate dehydrogenase from *Desulfovibrio vulgaris* Hildenborough, *FEMS Microbiol.*
28 553 *Lett.*, 1995, **133**, 143-149.
- 29 554 46. S. M. da Silva, C. Pimentel, F. M. Valente, C. Rodrigues-Pousada and I. A. Pereira, Tungsten
30 555 and molybdenum regulation of formate dehydrogenase expression in *Desulfovibrio vulgaris*
31 556 Hildenborough, *J. Bacteriol.*, 2011, **193**, 2909-2916.
- 32 557 47. H. G. Enoch and R. L. Lester, The purification and properties of formate dehydrogenase and
33 558 nitrate reductase from *Escherichia coli*, *J. Biol. Chem.*, 1975, **250**, 6693-6705.
- 34 559 48. J. J. Moura, C. D. Brondino, J. Trincao and M. J. Romao, Mo and W bis-MGD enzymes:
35 560 nitrate reductases and formate dehydrogenases, *J. Biol. Inorg. Chem.*, 2004, **9**, 791-799.
- 36 561 49. C. Pinske, S. Krüger, B. Soboh, C. Ihling, M. Kuhns, M. Braussemann, M. Jaroschinsky, C.
37 562 Sauer, F. Sargent, A. Sinz and R. Sawers, Efficient electron transfer from hydrogen to benzyl
38 563 viologen by the [NiFe]-hydrogenases of *Escherichia coli* is dependent on the coexpression of
39 564 the iron-sulfur cluster-containing small subunit, *Arch. Microbiol.*, 2011, **193**, 893-903.
- 40 565 50. S. Rivers, E. McNairn, F. Blasco, G. Giordano and D. Boxer, Molecular genetic analysis of
41 566 the moa operon of *Escherichia coli* K - 12 required for molybdenum cofactor biosynthesis,
42 567 *Mol. Microbiol.*, 1993, **8**, 1071-1081.
- 43 568 51. G. Schwarz, R. R. Mendel and M. W. Ribbe, Molybdenum cofactors, enzymes and pathways,
44 569 *Nature*, 2009, **460**, 839-847.
- 45 570 52. A. Kublik, D. Deobald, S. Hartwig, C. L. Schiffmann, A. Andrades, M. von Bergen, R. G.
46 571 Sawers and L. Adrian, Identification of a multi-protein reductive dehalogenase complex in
47 572 *Dehalococcoides mccartyi* strain CBDB1 suggests a protein-dependent respiratory electron
48 573 transport chain obviating quinone involvement, *Environ. Microbiol.*, 2016, **18**, 3044-3056.
- 49 574 53. J. S. Sousa, F. Calisto, J. D. Langer, D. J. Mills, P. N. Refojo, M. Teixeira, W. Kühlbrandt, J.
50 575 Vonck and M. M. Pereira, Structural basis for energy transduction by respiratory alternative
51 576 complex III, *Nature Communications*, 2018, **9**, 1728.
- 52 577 54. S. S. Venceslau, R. R. Lino and I. A. C. Pereira, The Qrc membrane complex, related to the
53 578 alternative complex III, is a menaquinone reductase involved in sulfate respiration, *J. Biol.*
54 579 *Chem.*, 2010, **285**, 22774-22783.

- 1
2
3 580 55. K. A. Datsenko and B. L. Wanner, One-step inactivation of chromosomal genes in
4 581 *Escherichia coli* K-12 using PCR products, *Proceedings of the National Academy of Sciences*,
5 582 2000, **97**, 6640-6645. View Article Online
DOI: 10.1073/pnas.97.13.6640
- 6 583 56. M. J. Casadaban, Transposition and fusion of the lac genes to selected promoters in
7 584 *Escherichia coli* using bacteriophage lambda and Mu, *J. Mol. Biol.*, 1976, **104**, 541-555.
- 8 585 57. T. Baba, T. Ara, M. Hasegawa, Y. Takai, Y. Okumura, M. Baba, K. A. Datsenko, M. Tomita,
9 586 B. L. Wanner and H. Mori, Construction of *Escherichia coli* K - 12 in - frame, single - gene
10 587 knockout mutants: the Keio collection, *Mol. Syst. Biol.*, 2006, **2**, 2006 0008.
- 11 588 58. M. D. Redwood, I. P. Mikheenko, F. Sargent and L. E. Macaskie, Dissecting the roles of
12 589 *Escherichia coli* hydrogenases in biohydrogen production, *FEMS Microbiol. Lett.*, 2008, **278**,
13 590 48-55.
- 14 591 59. T. Schubert, L. Adrian, R. G. Sawers and G. Diekert, Organohalide respiratory chains:
15 592 composition, topology and key enzymes, *FEMS Microbiol. Ecol.*, 2018, **94**, fiy035-fiy035.
16 593

594 **Tables**View Article Online
DOI: 10.1039/C9MT00009G595 **Table 1** *E. coli* mutant strains used for metal analysis

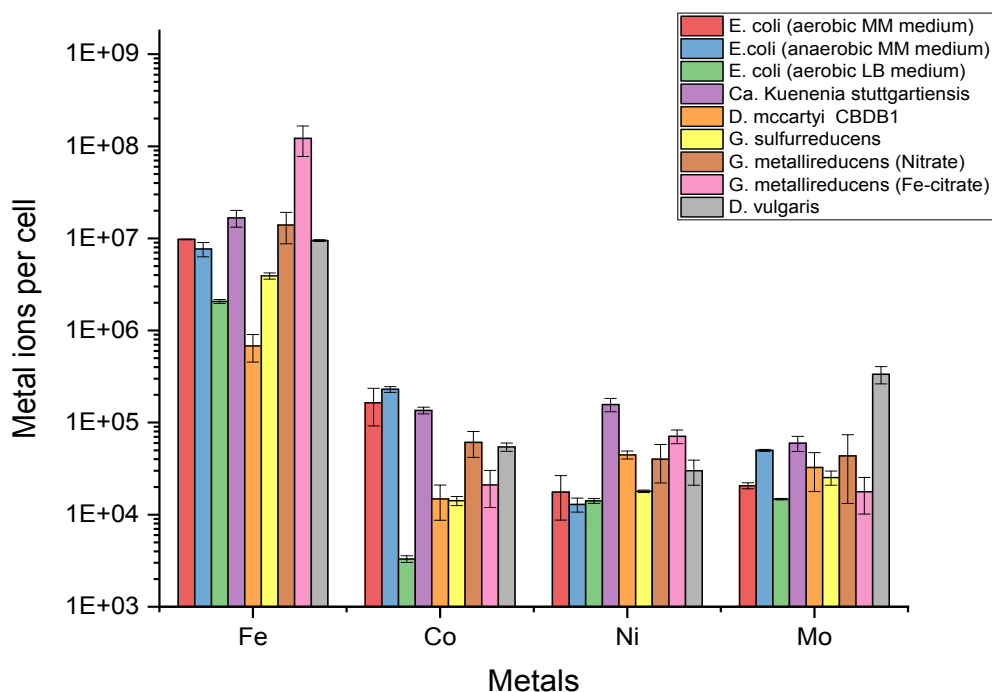
No.	Mutant Name	Description
1	BW25113	Wild-type <i>E. coli</i> strain: K12 derivative, $\Delta araBAD$, $\Delta rhaBAD$ ⁵⁵
2	MC4100	Wild-type <i>E. coli</i> strain F-, [araD139] (<i>argF-lac</i>)U169 <i>ptsF25 deoC1 relA1 flbB5301 rspL150</i> ⁵⁶
3	JW3443 $\Delta nikC$	BW25113 but $\Delta nikC$ Kan ^R ⁵⁷
4	JW3445 $\Delta nikE$	BW25113 but $\Delta nikE$ Kan ^R ⁵⁷
5	JW1328 Δfnr	BW25113 but Δfnr Kan ^R ⁵⁷
6	MC4100 $\Delta moaA$	MC4100 but $\Delta moaA$ Kan ^R (Kind gift from N. Dragomirova)
7	FTD147	MC4100 with deletion mutations in catalytic subunits of three [NiFe] hydrogenase subunits (\DeltahyaB , \DeltahybC , \DeltahycE) ⁵⁸
8	FTD147 + pASK-hybC	FTD147 with pASK-hybC (Amp ^R), which overproduces HybC, the large subunit of [NiFe] hydrogenase 2 ⁴⁹
9	FTD150 $\Delta selB$	MC4100 with knockout of three hydrogenase subunits (\DeltahyaB , \DeltahybC , \DeltahycE), $\DeltahyfB-R$ and the $\Delta selB$ gene, encoding the SelB translation factor ²¹
10	FTD150 $\Delta selB$ + pomeAB ^a	FTD150 $\Delta selB$ with pomeAB (Cm ^R), which overproduced the molybdoprotein subunit OmeA (Kind gift from S. Hartwig)

596 ^a The subunits of the originally named CISM enzyme from *D. mccartyi* have been recently renamed as
597 OmeA and OmeB.⁵⁹

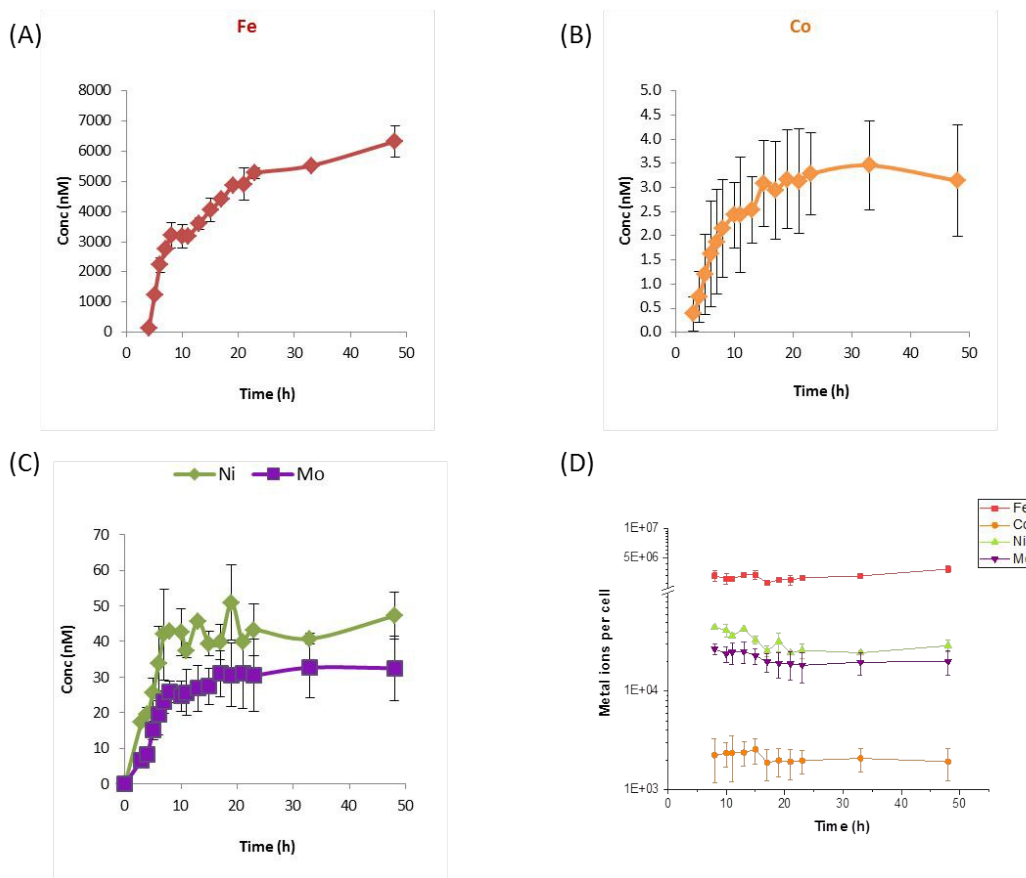
598 **Table 2** Isotopes selected for quantification of the target metals, their limit of detection (LOD)
599 and background equivalent concentration (BEC).

Metal isotope	LOD (nM)	LOD (ng L ⁻¹)	BEC (nM)
⁵⁶ Fe	2.68	150	17.41
⁵⁹ Co	0.02	1	0.08
⁶⁰ Ni	0.98	59	1.29
⁹⁵ Mo	0.26	25	1.06

600
601

602 **Figures**View Article Online
DOI: 10.1039/C9MT00009G

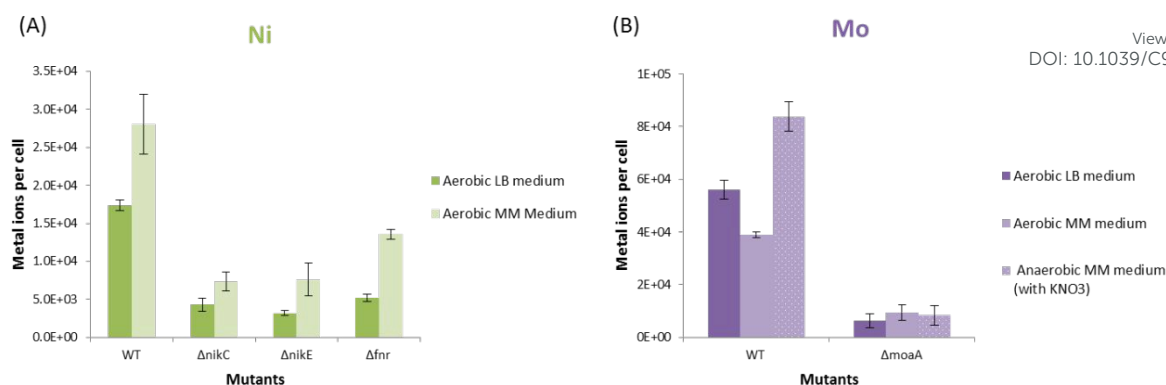
603
604 **Fig. 1** Fe, Co, Ni and Mo content of whole cells of different bacteria as determined by ICP-MS.
605 All cells were analyzed in three biological replicates and data are plotted as means \pm SD. Each
606 biological replicate was analyzed in three independent technical measurements and the mean was
607 further used.



View Article Online
DOI: 10.1039/C9MT00009G

608

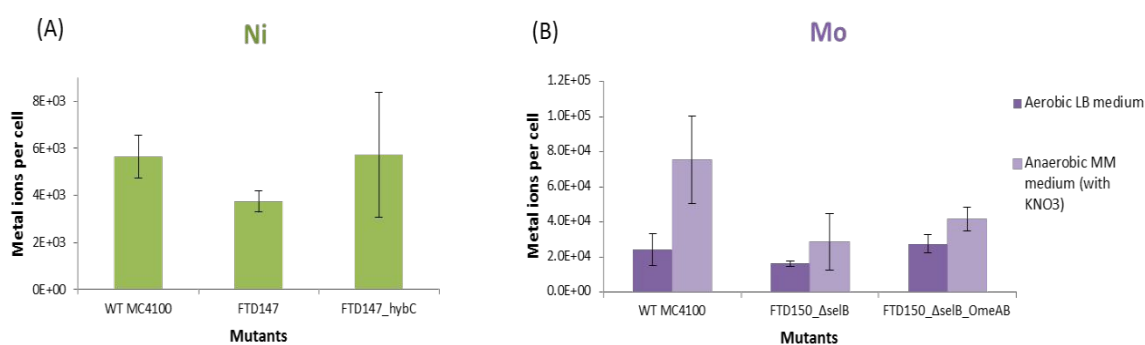
609 **Fig. 2** Metal content of *E. coli* strain BW25113 after aerobic growth in LB medium for 48 h;
 610 (A-C) concentration of biomass-bound metals calculated to the culture volume at different time points;
 611 (D) same data as in A-C but data were related to the cell number in the culture to obtain absolute
 612 numbers of ions per cell. All values are means of three independent measurements \pm SD.



View Article Online
DOI: 10.1039/C9MT00009G

613

614 **Fig. 3** Ni and Mo content in systemic *E. coli* knockout mutants. (A) Ni content in the *E. coli*
615 wild-type strain BW25113 (WT) and in the mutants $\Delta nikC$, $\Delta nikE$ and Δfnr , grown aerobically in LB
616 medium or aerobically in minimal medium (MM) A significant difference ($p^{**} < 0.01$) was observed
617 for all the mutant strains ($\Delta nikC$, $\Delta nikE$ and Δfnr) against wild-type strain. (B) Mo content in the wild-
618 type strain BW25113 and in a $\Delta moaA$ mutant, grown aerobically in LB medium, aerobically in MM or
619 anoxically in MM with KNO_3 as terminal electron acceptor. A significant difference ($p^{**} < 0.01$) was
620 observed for $\Delta moaA$ mutant against wild-type strain. The data show means of biological triplicates \pm
621 SD.



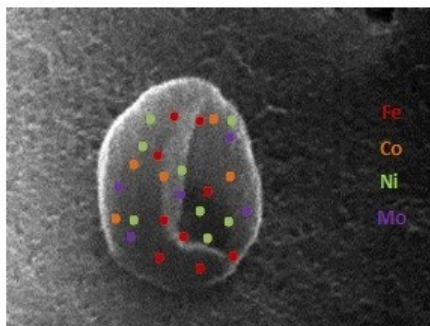
622

623 **Fig. 4** Ni and Mo content in structural gene mutants. (A) Ni content in the wild-type strain MC4100, a
624 mutant missing three subunits $\Delta hyaB$, $\Delta hybC$, $\Delta hycE$ of a [NiFe] hydrogenase (FTD147), and the
625 same mutant FTD147 overexpressing $hybC$ (FTD147_HybC). However, the difference between wild-
626 type strain and FTD147 mutant ($p = 0.07$), and the difference between FTD147 mutant and

1
2 627 FTD_hybC mutant ($p = 0.06$) was statistically not significant. (B) Mo content in the wild-type strain
3 628 MC4100, in a strain mutated in the genes encoding the catalytic subunits of all four hydrogenases, and
4 629 with a defect in synthesis of all three formate dehydrogenase genes due to deletion of *selB*
5 630 (FTD150_Δ*selB*), and the same strain FTD150_Δ*selB* mutant heterologously overproducing OmeA
6 631 and OmeB from *Dehalococcoides mccartyi* strain CBDB1.^{30, 52} OmeA contains a molybdopterin
7 632 binding-site. However, the difference between wild-type strain and FTD150_Δ*selB* mutant ($p =$
8 633 0.142), and the difference between FTD150_Δ*selB* mutant and FTD150_Δ*selB*_OmeAB mutant ($p =$
9 634 0.171) was statistically not significant. The data show means of biological triplicates \pm SD.

View Article Online
DOI: 10.1039/C9MT00009G

Bacterial cell



Metals measurement



234x106mm (72 x 72 DPI)

1
2
3
4
5
6
7
8
9
10
11
12
13
14
15
16
17
18
19
20
21
22
23
24
25
26
27
28
29
30
31
32
33
34
35
36
37
38
39
40
41
42
43
44
45
46
47
48
49
50
51
52
53
54
55
56
57
58
59
60